

Article

Defects Inspection in Wires by Nonlinear Ultrasonic-Guided Wave Generated by Electromagnetic Sensors

Junpil Park ¹, Jaesun Lee ², Junki Min ³ and Younho Cho ^{1,*}¹ School of Mechanical Engineering, Pusan National University, Busan 46241, Korea; jpp@pusan.ac.kr² School of Mechanical Engineering, Changwon National University, Changwon 51140, Korea; jaesun@changwon.ac.kr³ Gimhae Industry Promotion & Bio-Medical Foundation, Gimhae 50989, Korea; mjk6412@pusan.ac.kr

* Correspondence: mechcyh@pusan.ac.kr; Tel.: +82-51-510-2323

Received: 26 May 2020; Accepted: 25 June 2020; Published: 28 June 2020



Featured Application: The second harmonic measurement method using EMAT proposed in this paper has established a system that can detect microdefects in wires without destroying objects before wire processing.

Abstract: Steel wires are widely used as raw materials for spring valves in engines. Considering the quality and safety issues of their structure, there is a demand to develop nondestructive inspection approaches to detect initial damages in steel. In this study, nonlinear ultrasonic-guided waves generated by an electromagnetic acoustic transducer (EMAT) were used to inspect the defects in steel wires. As one of the noncontact testing methods, the use of EMAT has significant advantages to decrease the nonlinearity induced by instruments and transducer contact condition. The principles of design and manufacturing of EMAT are first introduced. The fundamental theory of nonlinear guided waves is also briefly discussed in this investigation. Phase-matched guided wave modes were generated and measured by using EMAT. Variations of acoustic nonlinearity corresponding to existing defects in specimens were obtained. A scanning electron microscope (SEM) was used to check the existence of microdefects in specimen. The results indicate that the use of EMAT can be an effective means to generate and measure nonlinear ultrasonic-guided waves for inspection of microdefects.

Keywords: steel wire rod; nonlinear ultrasonic; EMAT; guided wave

1. Introduction

Steel wire rods are used as raw materials for various mechanical components. This research can be applied to the steel wires, raw material of valve springs and have an influence on keeping smooth cycle motion in a gasoline engine. Under periodic fatigue state, failure of spring valves may occur before expectation of fatigue failure. Therefore, we need a reliable method for steel wires that can evaluate microdefects or early stage damage detection. Up to now, for the research work related with this study not so many articles were published. Gao et al. developed nondestructive evaluation (NDE) techniques using magnetic flux for macro defect [1].

The geometric shape of steel wires before processing of valve springs is cylindrical such as rod and solid shaft. Considering shape characteristics, guided waves have been applied to efficiently inspect long specimens such as wire rods. Research on guided ultrasound has been going on for a long time, but it has not progressed actively due to the complexity of theory and the variety of wave modes.

Gazis performed basic guided ultrasonic analysis of cylindrical structures [2,3]. Based on this, the test for guided ultrasound was started by Rose and Cawley's research works [4,5].

The nonlinear technique has the advantage that it can examine the microstructural changes in the nonlinear elastic section. It is based on information of distance, time and velocity of ultrasonic wave used in linear technique. In addition, the acquired ultrasonic signal is further analyzed in the frequency domain. The acquisition method of this technique is as follows: Information on the defect can be obtained by comparing the change at the second or third harmonic frequency. Through this, the internal microdefect can be diagnosed early. It is also possible to predict the life expectancy based on quantitative results. Buck et al. [6] conducted a study on the change of function of the stress and the second harmonic in which the transition occurs in the material. Subsequently, Jacobs and colleagues [7–9] studied the plasticization of materials using nonlinear guided ultrasound. Furthermore, according to using acoustic nonlinear guided wave technique, phase-matching mode is required to generate higher order harmonic amplitude. The basic concept of this research, concerning which factor is related with phase velocity and group velocity, has been improved by M. Deng [10,11].

EMAT is a noncontact technique. Research on EMAT has been conducted by M. Hiaro and H. Ogi of Osaka University [12–14]. Quantitative changes of physical nonlinearity should be measured by ultrasonic nonlinear method. Therefore, there is a need to continuously carry out experiments under the same conditions. That is, the same experimental apparatus and conditions are required to minimize the influence of the nonlinearity of the system. At this time depending on the contact conditions of the excitation and receiving transducers the reliability of this experiment may be greatly affected. This may change the nonlinearity. Therefore, to overcome the nonlinearity, a noncontact EMAT was applied.

Currently, research on microdefects in the material is proceeding smoothly by combining the contact method and the nonlinear method. However, the contact test method using piezoelectric transducer (PZT) requires a certain size of contact area, but it is impossible to test using PZT in a circular form in the case of the wire rod studied in this study. In addition since the PZT patch requires a contact medium such as an ultrasonic couplant, the signal is irregular depending on the amount or contact strength of the contact medium, so reproducibility is not constant when performing repeated experiments. Therefore, research using noncontact technology is necessary, but the result of the research is insufficient. In particular, there have been no reports on the application of the noncontact technique to the internal microdefects of steel wire rods. Therefore, this study applies the nonlinear method, guided wave and noncontact method.

Steel wire rod, which is the raw material of the engine piston valve spring, is typically manufactured from three materials. The nonlinear tendency according to the property of each material was analyzed to secure the suspected defective area. Flexible, torsional and longitudinal modes exist for guided waves in cylindrical structures such as piping and wire rods. Longitudinal mode is applied to ensure smooth secondary harmonics. In addition, we tried to obtain the reliability of the experimental results by setting the same geometric conditions. The nonlinear tendency of each specimen can be grasped through experiments. According to the result of the experiment, the suspected defect area was secured. This study provides a technical and academic understanding of nonlinear guided wave. By using noncontact ultrasonic technique rather than contact acoustic nonlinear guided waves, we can study for the purpose of precise diagnosis.

2. Nonlinear Guided Waves

2.1. Nonlinear Ultrasonic Test

The method for detecting nonlinearity in a material is to send and receive induced ultrasonic wave at a specific distance from the material. After the nonlinearity of the material propagates at a

certain distance, the underlying frequency wave is distorted to produce a higher harmonic [15–21]. For guided wave, the acoustic nonlinearity can be written as shown in Equation (1).

$$\beta = \frac{8}{K^2 a} \frac{A_2}{A_1^2} f \tag{1}$$

where a is the wave propagation distance and f is a frequency independent function. In addition, the ratio A_2/A_1^2 with the relative acoustic nonlinear parameter β' applied in this research is considered as a measure of acoustic nonlinearity, where A_1 and A_2 are the measured amplitudes of the fundamental and second harmonics.

$$\beta' = \frac{A_2}{A_1} \propto \beta a \tag{2}$$

The relative acoustic nonlinear parameter increases linearly as a function of propagation distance. The cumulative effect of the second harmonic amplitude is a great advantage for detection in experiment. It is found that second harmonic amplitude linearly grows with propagation distance, when there are synchronism and nonzero power flux. If the wave mode chosen satisfies these two conditions, the second harmonic amplitude will be cumulative. Even a series of double frequency wave components will be generated by the driving sources of nonlinearity. In practice, interest is focused on the second harmonic generation with the cumulative effect, since the cumulative second harmonic wave plays a dominant role after second harmonics propagating some distance.

Figure 1a,b shows the typical waveform of the received signal and its spectrum. The received time domain signal is processed in the frequency domain with the fast Fourier transform (FFT) to obtain its spectrum. Figure 1b shows the fundamental frequency and the second harmonic.

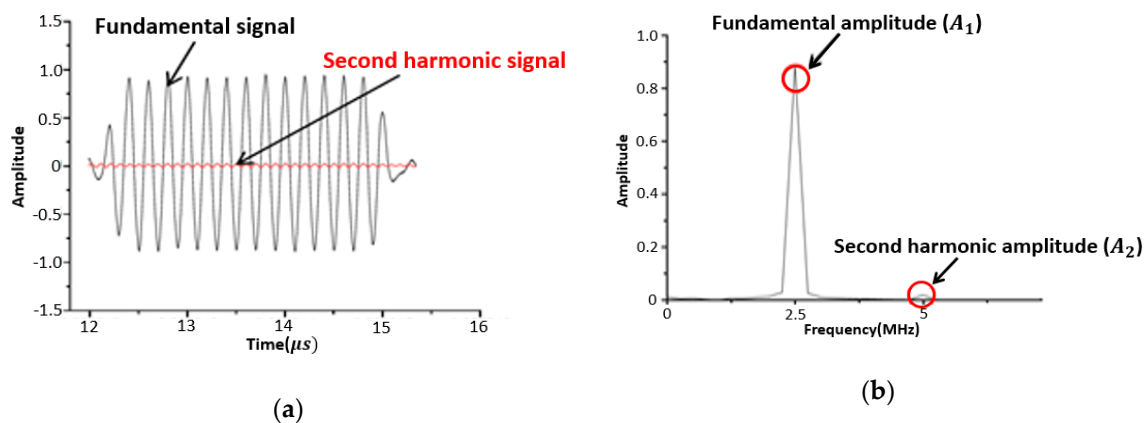


Figure 1. Typical received signal. (a) Time-domain waveform; (b) Fourier spectra of the fundamental and second harmonic signal.

As indicated in Equations (1) and (2), the normalized nonlinear parameter can be calculated with Equation (2) by using the amplitudes of the fundamental and the second harmonic modes.

Figure 2 shows the nonlinear parameters according to the propagation distance. The cumulative effect means that the nonlinearity increases with distance under certain frequency conditions. The double frequency mode which satisfies a specific condition such as the expression shown in the diagram is selected based on the frequency.

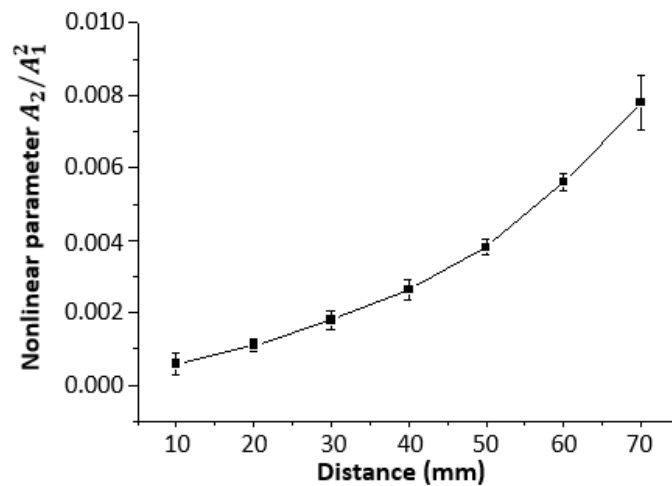


Figure 2. Nonlinear parameters according to distance.

2.2. EMAT

EMAT is composed of a generating coil for generating an eddy current of the electromagnet and the transmission and a receiving detecting coil. When the probe is approached to the metal specimen, the inside of the specimen is affected by the electromagnet. As Shown in Figure 3, the eddy current is formed on the surface of the specimen by an alternating current flowing in the generating coil inside the probe. Lorentz force is generated between the eddy current and the low power line, and mechanical displacement occurs on the surface of the specimen. This mechanical displacement is called ultrasound.

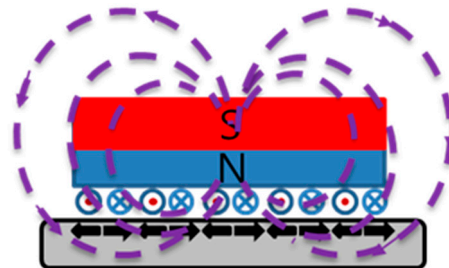


Figure 3. Principle of electromagnetic acoustic transducer (EMAT) with magnetic flux.

The purpose of this study was to investigate the nonlinearity of materials by inducing an ultrasonic wave in the longitudinal mode in steel wire rod. The permanent magnet was magnetically biased in the axial direction on the specimen. Then, when the coil was wound in the circumferential direction and the current was applied, the longitudinal mode of the guided ultrasonic wave was generated in the cylindrical structure such as the pipe or the wire rod.

EMAT was generated by Lorentz force effect in meander coil. The alternative current induce in the coil and the magnetic field is built in coil by high-power permanent magnet. Here J is eddy currents field and B is the magnetic field. The Lorentz force is generated by the eddy currents and magnetic field

$$\vec{F} = \vec{J} \times \vec{B} \tag{3}$$

As shown in Figure 4, the geometry used for describing the reception of EMAT is considering various factors. Equation (3) explain the relationship between magnetic field and eddy current. The influence of magnetic field for inducing eddy current is indicated by Equations (4) and (5). Produce a voltage pick up by receiving coil is Equation (6). EMAT does not require a contact medium in flaw detection. As a noncontact method using electromagnetic, it shows higher performance than

PZT for measuring nonlinearity of materials. However, it should be considered that the receiving sensitivity is lower than PZT.

$$\begin{aligned} E_{ed} &= v \times B & \vec{F} &= \vec{J} \times \vec{B} \\ J_{ed} &= \sigma \times E_{ed} \end{aligned} \tag{4}$$

$$\begin{aligned} \nabla^2 A_0 &= j\omega\sigma_0\mu_0 A_0 \\ \nabla^2 A_1 &= -\omega^2\sigma_1\mu_1 A_1 & \vec{F} &= \vec{J} \times \vec{B} \\ \nabla^2 A_2 &= j\omega\sigma_2\mu_2 A_2 \\ \nabla^2 A_3 &= j\omega\sigma_3\mu_3 A_3 \end{aligned} \tag{5}$$

$$\begin{aligned} E_r &= -\frac{\partial A}{\partial t} & \vec{F} &= \vec{J} \times \vec{B} \\ V_r &= N \times l \times E_r \end{aligned} \tag{6}$$

where v is the velocity of particle vibration, B is the static magnetic field, σ is the conductivity of the test piece, E_{ed} and J_{ed} are the induced electric field and the induced eddy current sheet due to the particle vibration at the depth z_{ed} respectively.

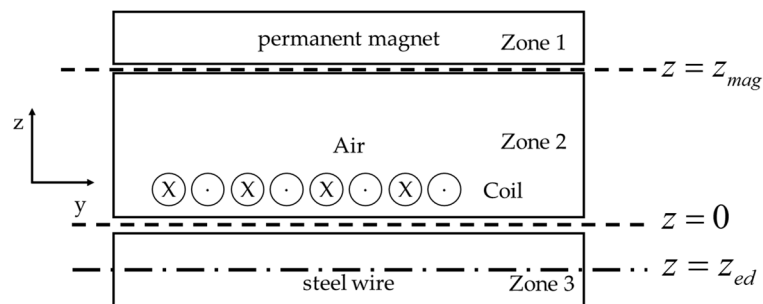


Figure 4. Geometry of steel wire and EMAT.

3. Experiments

Three different kinds of specimens with total 9 samples were tested in this investigation. As shown in Figure 5, the size information of the three specimens was the same, but there were differences in material properties and tensile strength. Detailed information of the samples can be found in in Table 1.



Figure 5. Specimens of steel wire rods.

Table 1. Material properties of specimens.

| List | Material Name | | |
|-----------------------|-----------------------------|-----------------------------|-----------------------------|
| | SWOSC-V | SWOSC-VHV | SWOSC-VHS |
| Line diameter | 3.2 mm | | |
| Length | 322 mm | | |
| Density | 787.4 g/mm ³ | | |
| Modulus of elasticity | 206 kN/mm ² | | |
| Yield stress | 0.9 × Tensile Strength | | |
| Tensile strength | 1860–2010 N/mm ² | 2010–2160 N/mm ² | 2110–2210 N/mm ² |
| C content | 0.51–0.59 | 0.63–0.68 | 0.63–0.68 |
| Si content | 1.20–1.60 | 1.20–1.60 | 1.80–2.20 |
| Mn content | 0.50–0.80 | 0.50–0.80 | 0.70–0.90 |

The frequency and modes were selected by frequency multiply wire thickness ($f \times d$). Phase matching must be performed through the dispersion curve. The conditions for generation of second harmonic in a cylindrical structure such as wire rod and pipe are as follows [13].

The power flux at the first harmonic should not be 0 in the second harmonic frequency range. ($f_n^{surf} + f_n^{vol} \neq 0$)

Phase and group velocities of the first and second harmonics should be the same through phase matching ($k_n^* = 2k$).

Figure 6 shows the dispersion diagram of steel wire rod. It can be confirmed that the phase velocity and the group velocity were the same at $4 \text{ MHz} \cdot \text{mm}$, which was a double frequency of $2 \text{ MHz} \cdot \text{mm}$. Through this phase-matching, we could use a nonlinear guided wave technique. L_1 ($f \cdot d = 2 \text{ MHz} \cdot \text{mm}$) and L_2 ($f \cdot d = 4 \text{ MHz} \cdot \text{mm}$) were selected because the resulted of the L_1 and L_2 modes were clearer for the second harmonic component than the other modes.

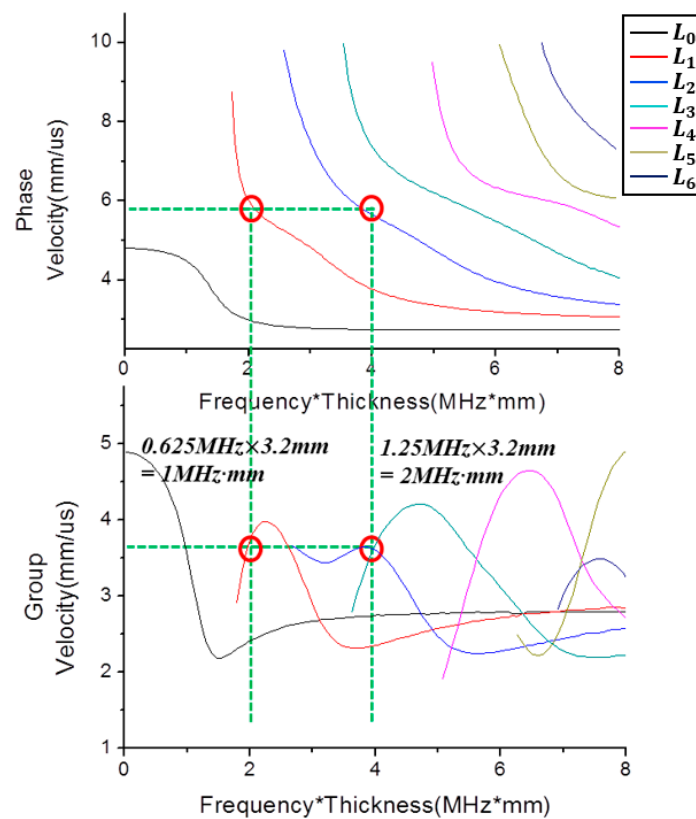


Figure 6. Dispersion curve of steel wire rod.

EMAT was designed and manufactured through impedance and LC-matching. Impedance matching means to eliminate the phase difference by minimizing reflection or loss of input power by buffering impedance difference at input and output. Selecting the appropriate inductor and capacitor element values through Equation (7) and choosing the resonance frequency is called LC-matching.

$$Z = R + j\omega L + \frac{1}{j\omega C} \vec{F} = \vec{J} \times \vec{B} \tag{7}$$

The frequency at which the imaginary part becomes 0 in the Equation (7) through matching between the inductor (L) and the capacitor (C) is called a resonance frequency. Figure 7 shows the resonance frequency due to LC-matching of the capacitor and the inductor.

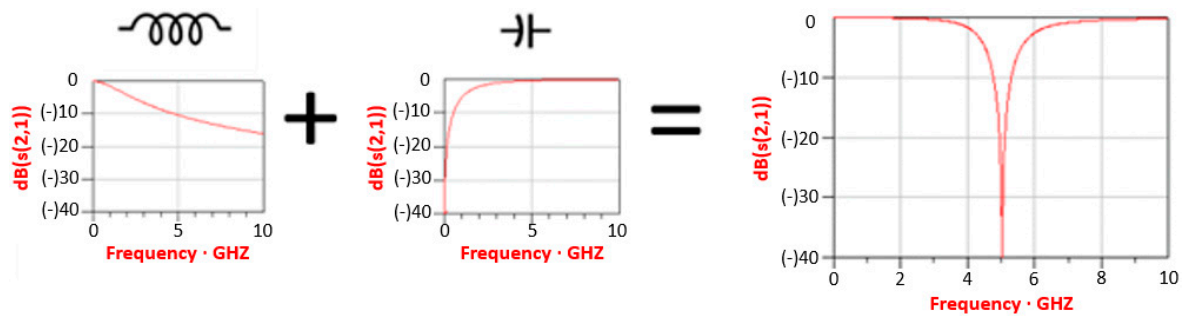


Figure 7. Resonant frequency setting by LC-matching of capacitor and inductor.

In order to realize the inductance in the ultrasonic generating coil, a long meander coil was used in a limited space. A resonant circuit was constructed to maximize current flow in the meander coil. Figure 8 shows a meander coil with a wavelength of 0.38 mm.

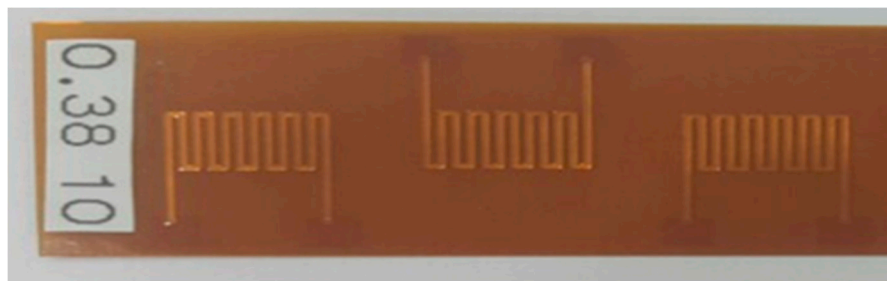


Figure 8. Meander coils with a wavelength of 0.38 mm.

Figure 9 shows the impedance-matching EMAT transducer used in this study. The EMAT was manufactured at 1 MHz as shown in Figure 10 and excited at 0.625 MHz. The wavelength ($\lambda = 5.82$ mm) of 1 MHz can be derived by substituting the desired frequency and longitudinal wave velocity ($C_{Steel}^L = 5.82$ mm/ μ s) in the steel into Equation (8).

$$\lambda = \frac{c}{f} \vec{F} = \vec{J} \times \vec{B} \tag{8}$$



Figure 9. Impedance-matched EMAT transducer.



Figure 10. Impedance matching.

Practically, 5.82 mm cannot be applied to steel wire with a diameter of 3.2 mm. It can be applied with lower wavelength as $\lambda/2, \lambda/4, \lambda/8$. Since 0.38 mm is an approximate value of $1/16$ of wavelength, EMAT was fabricated using 0.38-mm meander coil.

Experiments were conducted to investigate the behavior of nonlinear induced ultrasound. Figure 11 shows the experimental setup. The RITEC RAM-4000 was used as a tone-burst ultrasonic transmitter and receiver and it was processed by a pitch-catch method.

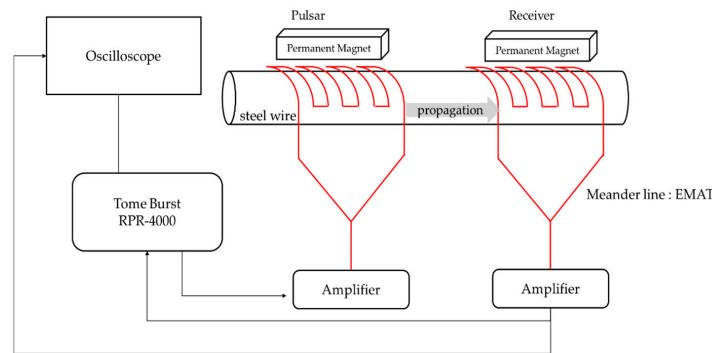


Figure 11. Experimental setup for using EMAT.

In order to obtain the reliability of the experimental results, the same geometric conditions were set, and two kinds of experiments were conducted. As shown in Figure 12, a meander line and permanent magnets were installed on the steel wire rod. As shown in Figure 13a, the first experiment was divided into four sections of 60 mm each, and the relative nonlinearity of each wire was confirmed. The second experiment was conducted by increasing the propagation distance by 60 mm as shown in Figure 13b. The schematic diagram of each experiment is shown in Figure 13. Experiments were conducted to determine whether defects could be detected through the relative nonlinearity.

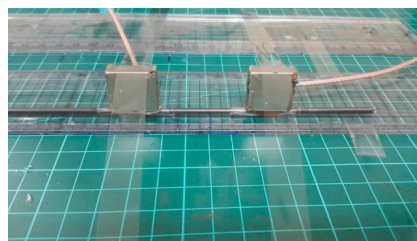


Figure 12. Setup of the meander line and permanent magnet on steel wire rod.

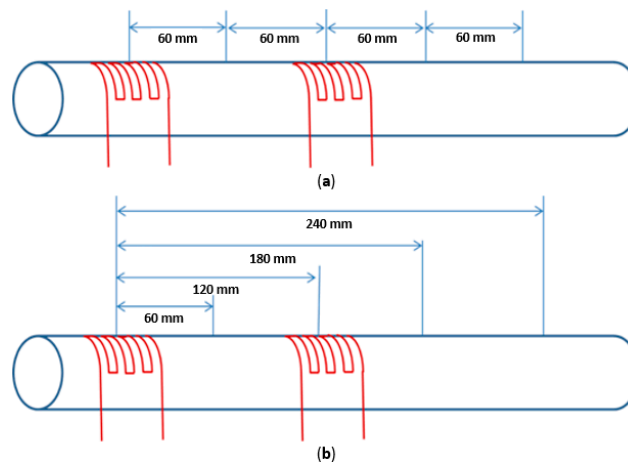


Figure 13. Schematic of experimental: (a) Experimental method with each detection area; (b) experimental method with increasing distance.

4. Results and Discussion

The relative nonlinearity of the fabricated EMAT sensor was measured for each specimen in the longitudinal direction of the steel wire. The relative nonlinearity tendency was studied. As mentioned above, the nonlinear guided wave technique is a technique to diagnose changes in material properties and microdefects by using harmonic components unlike the conventional technique. EMAT shows higher performance than PZT to measure nonlinearity of material because it does not need contact medium and uses electromagnetic in flaw detection. In case of using PZT, the error due to the individual difference of the experimenter cannot be ignored. Therefore, the method using EMAT is very appropriate. Figure 14 shows the signals for linear ultrasonic wave in three specimens. The time domain signal for each specimen can distinguish between the distance and the speed relative to the time, however, microdefects cannot be confirmed. In addition, the analysis of the modes showed that the L_1 mode was well implemented for SWOSC-V and SWOCS-VHV, but SWOSC-VHS was able to confirm that the various modes were mixed. Therefore, the experiment was conducted using a nonlinear guided ultrasonic technique using second harmonic.

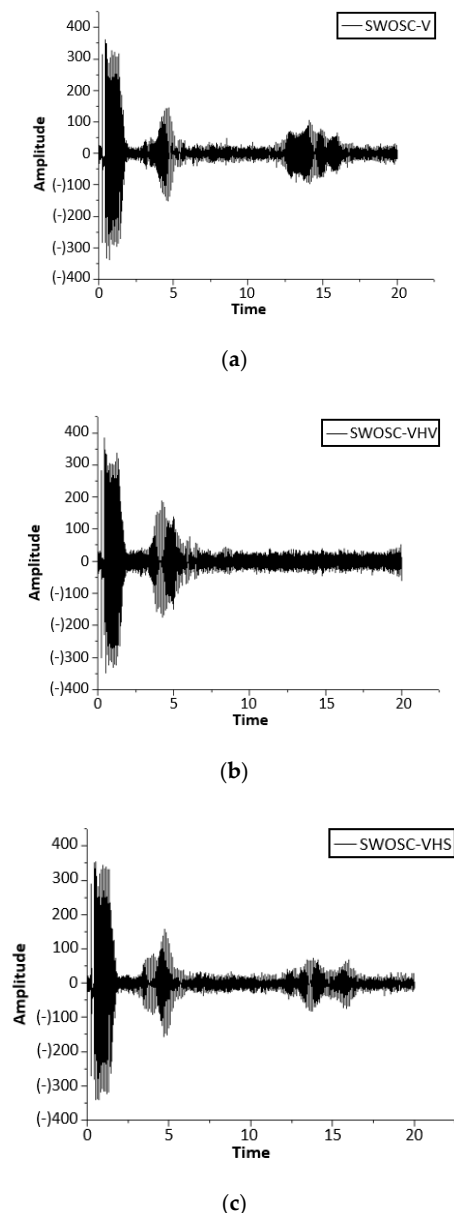


Figure 14. Time domain signal. (a) SWOSC-VHS #1; (b) SWOSC-VHV #2; (c) SWOSC-VHS #3.

The fundamental amplitude A_1 and second harmonic amplitude A_2 amplitude values can be derived by measuring the time domain signal of 60 mm intervals from three specimen for each material and then performing FFT. Substituting the derived A_1 and A_2 into Equation (2), nonlinear parameters can be obtained for each specimen. Figure 15 is the result of comparing the relative nonlinearity in each zone. In all three specimens of SWOSC-V, the relative nonlinearity increases with increasing propagation distance. The relative nonlinearity of all three specimens decreases at the propagation distance of 181–240 mm, which can be regarded as the material properties of the specimen. SWOSC-VHV also shows the same tendency of three specimens. However, SWOSC-VHS # 2 has a tendency to be different from the # 1 and # 3 specimens at 61–180 mm propagation distance. Three specimens with the same physical properties should show the same tendency toward in each section. However, since VWOSC-VHS #2 has a different tendency from the VWOSC-VHS #1 and #3 samples, it can be determined that there is some abnormality inside the material.

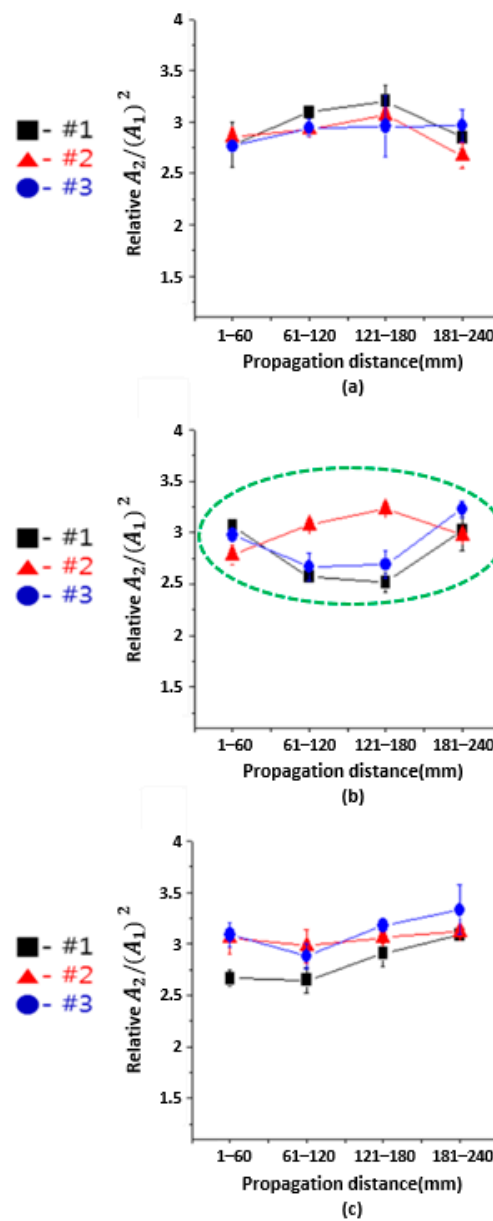


Figure 15. Relative nonlinearity for each detection area (a) Results of the three-specimen test in SWOSC-V (b) results of the three-specimen test in SWOSC-VHV (c) results of the three-specimen test in SWOSC-VHS.

Because of the tendency to suspect microscopic defects, additional experiments were conducted to ensure the reliability of the experimental data. Figure 16 is the relative nonlinearity with increasing distance, which was an additional experimental result. SWOSC-V and SWOSC-VHS could obtain a tendency for relative nonlinearity change as the distance increased. However, # 3 of SWOSC-VHV showed a large difference in relative nonlinear factor values from # 1 and # 2 at a propagation distance of 120 mm, but it was very difficult to be considered as a suspected defect region due to the agreement of the tendency for each specimen. At the propagation distance of 180 mm, SWOSC-VHH # 2 had the same tendency as the previous experimental results. A total of two experiments were used to consider suspected microdefects in SWOSC-VHV # 2 at a propagation distance of 180 mm.

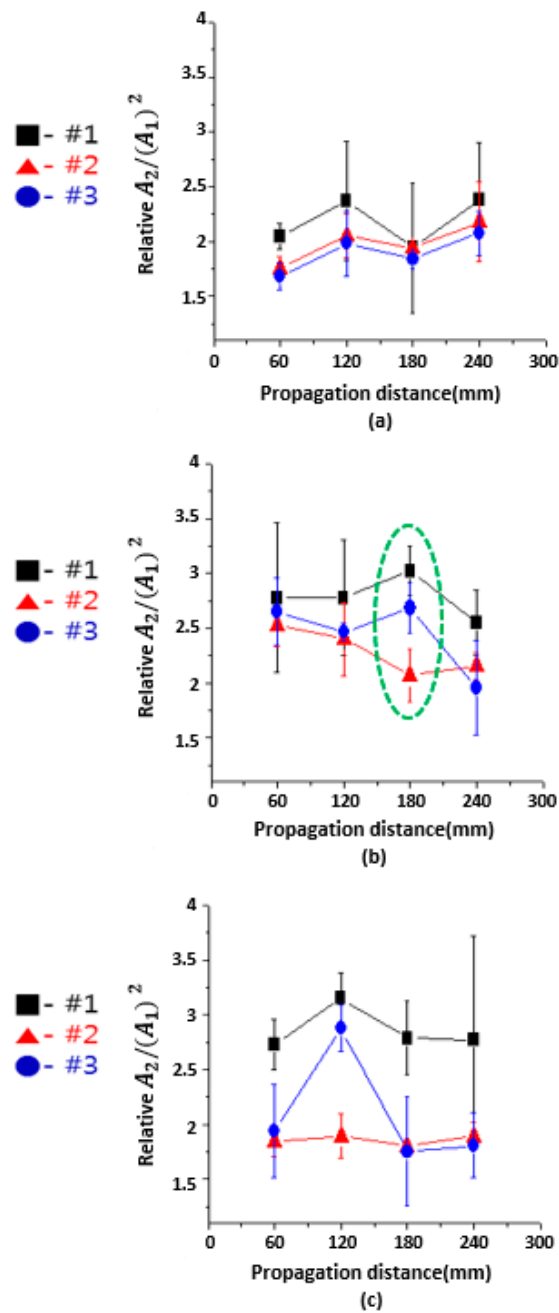


Figure 16. Relative nonlinearity variation of considering propagation distance (a) Results of the three-specimen test in SWOSC-V (b) results of the three-specimen test in SWOSC-VHV (c) results of the three-specimen test in SWOSC-VHS.

Figure 17 is cross-sectional photographs of microdefect suspected areas and defective free area. Figure 17b shows a clear difference in the distribution of microdefects compared to Figure 17a. This is consistent with the experimental results and SEM photographs. Therefore, it can be seen that the reliability of the experimental result was secured. Figure 18 shows the result of enlarged the micro defect.

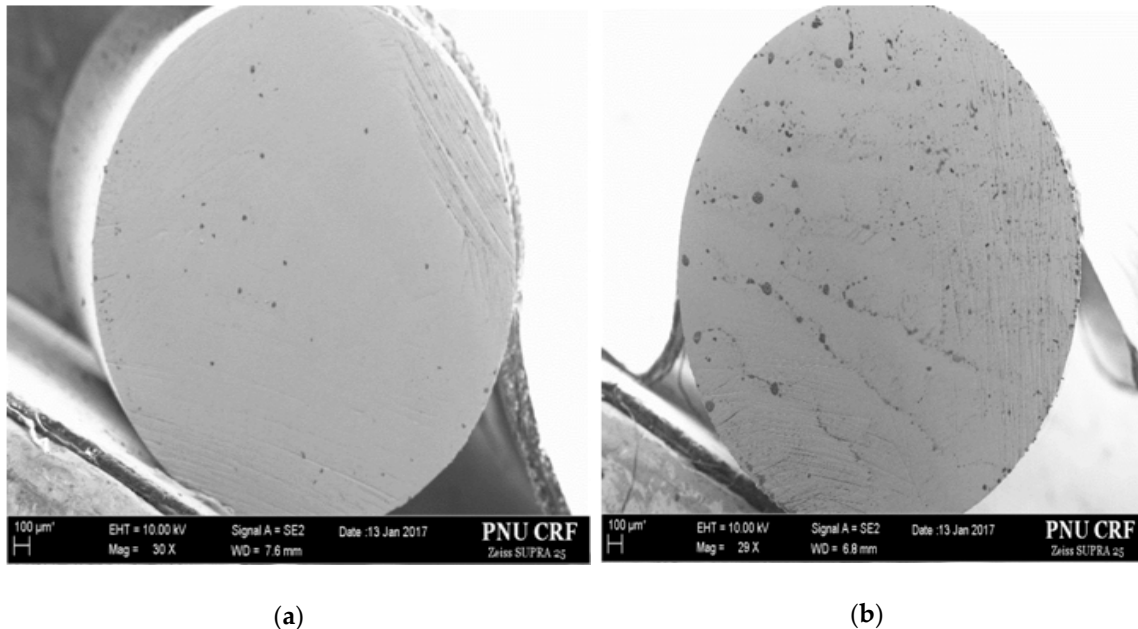


Figure 17. Comparison of SEM result for steel wire. (a) SWOSC-VHS #1: non-defect area; (b) SWOSC-VHS #2: defect area.

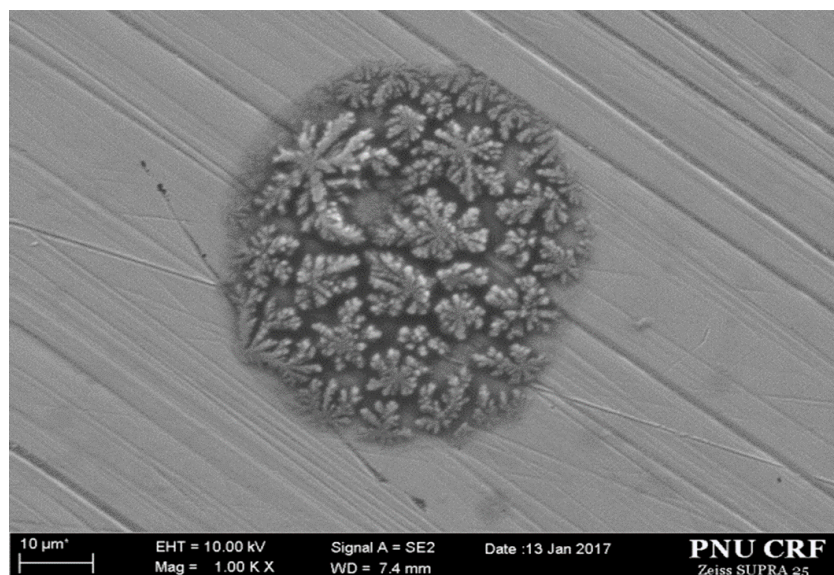


Figure 18. Enlarged microdefect.

The experimental results were not quantitative because the distance between the coils and the specimen changed finely when the reinstallation was repeated after separating the meander coil and the specimen from each other during the experiment. In other words, the lift-off changed. In order to solve this problem, we had to build a proper system to fix the meander coil and the specimen firmly. In addition, since the nonlinearity was very sensitive, the ultrasound path difference may have

occurred due to the minute scratches on the surface of the specimen, resulting in energy loss and affecting the damping coefficient. Therefore, it is necessary to acquire precision machined specimens.

5. Conclusions

In this study, the nonlinearity tendency of microdefects was investigated by applying guided wave and nonlinear method to steel wire using EMAT. The relative nonlinearity of each specimen is specific for each material. This is considered to be a characteristic of the content of elements constituting the material. Experimental results show that specimens with large errors and specimens without specimens exist. This is considered to be an error due to the distance between the meander coil and the specimen, that is, the lift-off, when the specimen and the coil are separated and remounted. SEM images were taken to verify the reliability of the experimental results. The results were very satisfactory. The possibility of diagnosing microdefects in steel wire production line was confirmed. In order to utilize the nonlinear technique, there is a need to acquire defect-free specimens. We have identified the need for a system that can acquire clear signals. However, there were experimental errors, there is no critical dispute in confirming the tendency for each specimen. It is possible to observe relatively the suspicion of microdefect. It is expected that quantitative evaluation of each specimen will be possible if the parameters of nonlinear factor are removed through a system which can fix the defect-free specimen and lift-off later. In addition, if this research technique is used, it is possible to quickly check noncontact for defects of steel wire rods passing through the inspection line, and to detect fine defects early before processing the steel wire rod to enhance the safety of the material. It was suitable for inspecting the initial fine defects in steel wires before spring processing by utilizing EMAT, a noncontact method without contact medium. The noncontact method is a method capable of minimizing the deformation of the signal that changes depending on the amount or compression state of the contact medium. If the technique is applied to the industrial site, it is judged that it will be possible to test for microdefects quickly and consistently.

Author Contributions: J.P. and J.M. designed and performed the experiments. J.L. and Y.C. conceived the original idea. J.P. developed the theory and performed the computations with support from J.L. and Y.C. verified the analytical methods. J.M. and J.L. wrote the draft study, J.P. completed the final study and Y.C. made the final review. All authors have read and agreed to the published version of the manuscript.

Funding: This work was supported by the Korean Evaluation Institute of Industrial Technology (KEIT) grant funded by the Korean government (MOTIE) (NO.10085576).

Acknowledgments: This research was carried out with the support of materials from Daewon Kang Up Co., Ltd.

Conflicts of Interest: The authors declare no conflict of interest.

References

1. Yan, X.; Zhang, D.; Pan, S.; Zhang, E.; Gao, W. Online nondestructive testing for fine steel wire rope in electromagnetic interference environment. *NDT E Int.* **2017**, *90*, 75–81. [[CrossRef](#)]
2. Gazis, D.C. Three dimensional investigation of the propagation of waves in hollow circular cylinders. *J. Acoust. Soc. Am.* **1959**, *31*, 568–573. [[CrossRef](#)]
3. Rose, J.L. *Ultrasonic Waves in Solid Media*; Cambridge University Press: Oxford, UK, 2004.
4. Rose, J.L. A baseline and vision of ultrasonic guided wave inspection potential. *J. Pres. Ves. Tech.* **2002**, *124*, 273–282. [[CrossRef](#)]
5. Lowe, M.J.S.; Alleyne, D.N.; Cawley, P. Defect detection in pipes using guided waves. *Ultrasonics* **1998**, *36*, 147–154. [[CrossRef](#)]
6. Buck, O. Harmonic generation for measurement of internal stress as produced by dislocation. *IEEE Trans. Sonics Ultrason.* **1976**, *SU-23*, 346–350. [[CrossRef](#)]
7. Shui, G.; Kim, J.Y.; Qu, J.; Jacobs, L. A new technique for measuring the acoustic nonlinearity of material using Rayleigh waves. *NDT E Int.* **2008**, *41*, 326–329. [[CrossRef](#)]
8. Kim, J.Y.; Qu, J.; Jacobs, L.J. Acoustic nonlinearity parameter due to micro-plasticity. *J. Nondestruct. Eval.* **2006**, *25*, 29–37. [[CrossRef](#)]

9. Pruell, C.; Kim, J.-Y.; Qu, J.; Jacobs, L.J. Evaluation of plasticity driven material damage using Lamb waves. *Appl. Phys. Lett.* **2007**, *91*, 231911. [[CrossRef](#)]
10. Deng, M. Cumulative second harmonic generation of Lamb mode propagation in a solid plate. *J. Appl. Phys.* **1999**, *85*, 3051–3058. [[CrossRef](#)]
11. Deng, M. Analysis of second-harmonic generation of Lamb waves propagating in layered planar structures with imperfect interfaces. *Appl. Phys. Lett.* **2006**, *88*, 221902. [[CrossRef](#)]
12. Hirao, M.; Ogi, H. Electromagnetic acoustic resonance and materials characterization. *Ultrasonics* **1977**, *35*, 413–421. [[CrossRef](#)]
13. Hirao, M.; Ogi, H.; Fukuoka, H. Resonance EMAT system for acoustoelastic stress measurement in sheet metals. *Rev. Sci. Instruments* **1993**, *64*, 3198–3205. [[CrossRef](#)]
14. Hirao, M.; Ogi, H. An SH-wave EMAT technique for gas pipeline inspection. *NDT E Int.* **1999**, *32*, 127–132. [[CrossRef](#)]
15. Li, W.; Deng, M.; Xiang, Y.X. Review on second-harmonic generation of ultrasonic guided waves in solid media (I): Theoretical analyses. *Chin. Phys. B* **2017**, *26*, 114302. [[CrossRef](#)]
16. Matlack, K.H.; Kim, J.-Y.; Jacobs, L.J.; Qu, J. Experimental characterization of efficient second harmonic generation of lamb wave modes in a nonlinear elastic isotropic plate. *J. Appl. Phys.* **2011**, *109*, 014905. [[CrossRef](#)]
17. Li, W.; Deng, D.; Cho, Y. Cumulative Second Harmonic Generation of Ultrasonic Guided Waves Propagation in Tube-Like Structure. *J. Comput. Acoust.* **2016**, *24*, 1650011. [[CrossRef](#)]
18. Kim, J.; Zhu, B.; Cho, Y. An experimental study on second harmonic generation of guided wave in fatigued spring rod. *J. Mech. Sci. Technol.* **2019**, *33*, 4105–4109. [[CrossRef](#)]
19. Li, W.; Jiang, C.; Qing, X.; Liu, L.; Deng, M. Assessment of low-velocity impact damage in composites by the measure of second-harmonic guided waves with the phase-reversal approach. *Sci. Prog.* **2019**, *103*, 103. [[CrossRef](#)] [[PubMed](#)]
20. Li, W.; Chen, B.; Qing, X.; Cho, Y. Characterization of Microstructural Evolution by Ultrasonic Nonlinear Parameters Adjusted by Attenuation Factor. *Metals* **2019**, *9*, 271. [[CrossRef](#)]
21. Li, W.; Cho, Y.; Li, X. Comparative Study of Linear and Nonlinear Ultrasonic Techniques for Evaluation Thermal Damage of Tube-Like Structures. *J. Korean Soc. Nondestruct. Test.* **2013**, *33*, 1–6. [[CrossRef](#)]



© 2020 by the authors. Licensee MDPI, Basel, Switzerland. This article is an open access article distributed under the terms and conditions of the Creative Commons Attribution (CC BY) license (<http://creativecommons.org/licenses/by/4.0/>).